This is the Pre-Published Version.
This is the peer reviewed version of the following article: Zhang, Y., Yang, P., Teng, H., Ng, H. D., & Wen, C. (2018). Transition between different initiation structures of wedge-induced oblique detonations. AIAA Journal, 56(10), 4016-4023 , which has been published in final form at https://doi.org/10.2514/1.J056831. © 2018 by the American Institute of Aeronautics and Astronautics, Inc. All rights reserved.

Transition Between Different Initiation Structures of Wedge-Induced Oblique Detonations

Yining Zhang*
Beijing Power Machinery Research Institute, 100074 Beijing, People's Republic of China
Pengfei Yang† and Honghui Teng‡
Beijing Institute of Technology, 100081 Beijing, People's Republic of China
Hoi Dick Ng§
Concordia University, Montreal, Quebec H3G 1M8, Canada
and
Chihyung Wen¶
Hong Kong Polytechnic University, Kowloon, Hong Kong, People's Republic of China

Oblique detonation waves (ODWs) have been widely studied due to their application potential for airbreathing hypersonic propulsion. Moreover, various formation structures of wedge-induced oblique detonation waves have been revealed in recent numerical investigations. Given the inflow conditions, the wave configuration is dependent on the wedge angle. Hence, any wedge-angle change will induce a transient ODW evolution to transition from one configuration to another. In this study, the transient development created by instantaneously changing the wedge angle is investigated numerically, based on the unsteady two-dimensional Euler equations and one-step irreversible Arrhenius chemical kinetics. The evolution caused by the abrupt wedge-angle change from one smooth initiation structure to another, both with a curved oblique shock/detonation surface at high-Mach-number regime, is investigated. Two processes are analyzed; the first consists of the downstream transition of the ODW initiation region the by decreasing the angle, and the second is the upstream transition by increasing the angle. In the downstream transition, the overall structure moves globally and readjusts continuously, generating an intermediate kinklike initiation structure. In the upstream transition, a localized reaction region forms and induces a more complex process, mainly derived from the different responding speeds of the oblique shock and detonation waves. To avoid the generation of the new localized explosion region, which causes an abrupt change in the initiation position and potentially affects the ODWE's stability and performance, it is suggested to vary the wedge angle in incremental steps within a certain time interval.

Nomenclature

E_a	=	activation energy
e	=	total energy
k	=	preexponential factor
$L_{1/2}$	=	half reaction zone length
M_0	=	flight Mach number
M_1	=	predetonation inflow Mach number
p	=	pressure
q	=	heat release of chemical reaction
R	=	universal gas constant
T	=	temperature
T_0	=	premixed mixture temperature
t	=	time
u	=	velocity in the x direction
v	=	velocity in the y direction
γ	=	ratio of specific heats
θ	=	wedge angle
λ	=	chemical reaction progress index
ρ	=	density
$\dot{\omega}$	=	chemical reaction rate

I. Introduction

FOR a supersonic combustible gas flow past a wedge, depending on the incoming flow condition and the wedge angle, an oblique shock wave (OSW) is attached to the wedge and may trigger the formation of an oblique detonation wave (ODW). The idea of harnessing a standing ODW for hypersonic airbreathing propulsion systems has long been considered and is still under investigation [1–4]. Although many theoretical investigations have provided the basic foundation for steady ODWs [5–8], the current research on ODW phenomenon has been toward attaining a better fundamental understanding of its transient formation structure and stability.

Over the past decades, many investigations have been performed that reveal different ODW formation structures. The classical structure of an oblique detonation wave stabilized over a wedge was revealed in the pioneering work of Li et al. [9,10] by means of numerical simulations and later confirmed experimentally by Viguier et al. [11]. This classical structure is composed of a nonreactive oblique shock, a set of deflagration waves, and the oblique detonation surface, all united on a multiwave point. The sketch of this structure is illustrated in Fig. 1a, which is referred to as the abrupt transition from OSW to ODW. A different type of formation structure has also been described in Fig. 1b, demonstrating that the transition may occur smoothly from a curved shock [12–14], rather than an abrupt transition through a multiwave point. The smooth transition usually appears in the cases of high Mach number M_1 and low activation energy E_a, without cellular structures near the initiation region. Recent studies also reveal more complex ODW formation structures of different wave configurations, with the induction region observed

*Senior Research Fellow, State Key Laboratory of Laser Propulsion and Application, P.O. Box 7208.
†Graduate Student, Department of Mechanics, School of Aerospace Engineering, No. 5, Zhongguancun South Street.
‡Professor, Department of Mechanics, School of Aerospace Engineering, No. 5, Zhongguancun South Street.
§Professor, Department of Mechanical, Industrial and Aerospace Engineering, 1515 Saint-Catherine Street West. Senior Member AIAA.
¶Professor, Department of Mechanical Engineering. Associate Fellow AIAA.

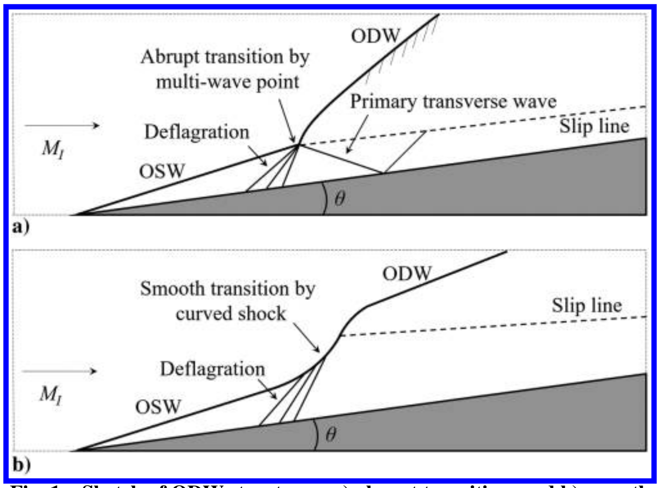

Fig. 1 Sketch of ODW structures: a) abrupt transition, and b) smooth transition.

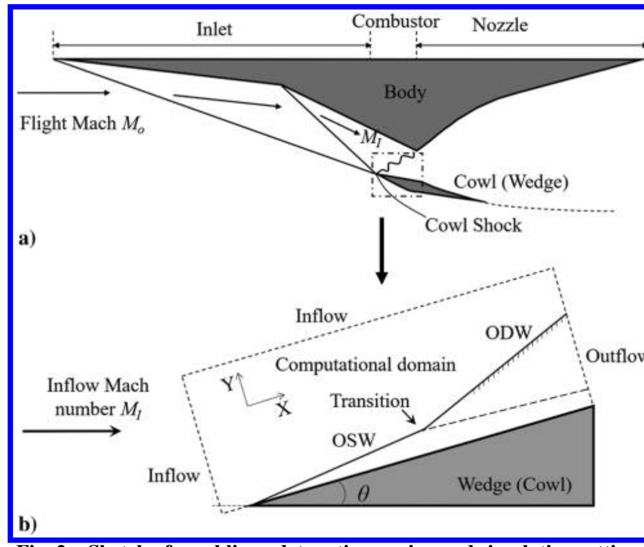

Fig. 2 Sketch of an oblique detonation engine and simulation settings.

to be ended by an internal Chapman–Jouguet (CJ) detonation wave rather than a set of deflagration waves at low inflow Mach number condition [15–20]. With regard to the established oblique detonation waves, a number of numerical investigations have demonstrated that the ODW is inherently unstable with fine-scale instability features on the oblique detonation surfaces similar to the unstable frontal structure of normal cellular detonations [13,21–26].

For ODW applications in propulsion systems, it is vital to assess the wave structure dynamics as well as its static configuration. Aforementioned studies [12–20] assume that the inflow is well premixed and uniform, which is seldom available in practical situations. Therefore, a number of recent studies have been carried out concerning the effect of mixture inhomogeneity of the premixed combustible gas flow on the ODW formation due to incomplete mixing [9,27–32]. These studies introduced large disturbances composed of a region with radical species or a spatial variation in the equivalence ratio of the flow. The ODW is generally found to be distorted by these disturbances, and in some cases, the formation is replaced by a more complicated structure. However, the effects of nonstationary inflow are not studied thus far to the authors' knowledge.

The present numerical study addresses the transitions between different ODW formation structures, which can be viewed as the simplest situation of the nonstationary inflow. It is often impossible to maintain the inflow conditions constant in practical engines, which may induce different ODWs, and some controlling parameters needs to be adjusted accordingly. Apart from the chemical control by changing the amount of fuel injection to vary the energetics of the combustible, a mechanical way to adjust the ODW structure in response to any incoming flow perturbation is by varying the wedge angle. As a first step to describe ODW engine performance in relation to wedge-angle variation, this work aims to investigate how one ODW formation structure evolves into another and the related flowfield dynamics. Two typical smooth ODW formation structures are first introduced, whose initiation positions are controlled by the wedge angle with the same incident or inflow Mach number. The dynamic transition process is induced by an instantaneous wedge-angle variation, and two kinds of processes are observed and analyzed.

II. Physical Model and Computational Method

A schematic of an ODW engine [33] and the wedge-induced oblique detonation is shown in Fig. 2. The combustible inflow reflects on the two-dimensional wedge, and high temperature may trigger exothermic chemical reactions and lead to the onset of an oblique detonation wave. As shown in Fig. 2a, the current study focuses only on the cowl region enclosed by the dashed lines with variable wedge angle. The inflow Mach number M_I is prescribed for the present simulation (i.e., the effect of impinging oblique shocks are not investigated). For the present numerical study, the computational domain bounded by the dashed zone is also shown in Fig. 2b, whose coordinates are aligned with the wedge surface. Previous numerical studies [10,12] indicate that the viscosity and boundary layer have little effect on this structure, except changing the boundary-layer thickness slightly. Hence, following most of the previous numerical studies [13–26], the present study is also based on the inviscid assumption. The nondimensional governing equations with a single-step, irreversible chemical reaction are of the form

$$\frac{\partial U}{\partial t}+\frac{\partial E}{\partial x}+\frac{\partial F}{\partial y}+S=0 \tag{1}$$

$$U=\begin{bmatrix}\rho\\ \rho u\\ \rho v\\ \rho e\\ \rho\lambda\end{bmatrix},\quad E=\begin{bmatrix}\rho u\\ \rho u^2+p\\ \rho uv\\ \rho u(e+p)\\ \rho u\lambda\end{bmatrix},\quad F=\begin{bmatrix}\rho v\\ \rho uv\\ \rho v^2+p\\ \rho v(e+p)\\ \rho v\lambda\end{bmatrix},\quad S=\begin{bmatrix}0\\ 0\\ 0\\ 0\\ \dot{\omega}\end{bmatrix} \tag{2}$$

with

$$e=\frac{p}{(\gamma-1)\rho}+\frac{1}{2}(u^2+v^2)-\lambda Q \tag{3}$$

$$p=\rho T \tag{4}$$

$$\omega=-k\rho(1-\lambda)\exp(-E_a/T) \tag{5}$$

All the flow variables have been made dimensionless by reference to the uniform unburned state ahead of the detonation front:

$$\rho=\frac{\tilde{\rho}}{\tilde{\rho}_0},\ p=\frac{\tilde{p}}{\tilde{\rho}_0},\ T=\frac{\tilde{T}}{\tilde{T}_0},\ u=\frac{\tilde{u}}{\sqrt{\tilde{R}\tilde{T}_0}},\ Q=\frac{\tilde{Q}}{\tilde{R}\tilde{T}_0},\ E_a=\frac{\tilde{E}_a}{\tilde{R}\tilde{T}_0} \tag{6}$$

For the chemical reaction, λ is the reaction progress variable, which varies between 0 (for unburned reactant) and 1 (for product). The reaction is controlled by the activation energy E_a and the preexponential factor k, and the latter is chosen to define the spatial and temporal scales. The governing equations are discretized on Cartesian uniform grids and solved with the Monotonic Upwind Scheme for Conservation Laws (MUSCL)–Hancock scheme with Strang's splitting. The MUSCL–Hancock scheme is formally a second-order extension to Godunov's first-order upwind method by constructing the Riemann problem on the intercell boundary [34]. The scheme is made total variation diminishing with the use of slope limiter MINBEE, and the Harten-Lax-van Leer-Contact (HLLC) approximate solver is used for the Riemann problem.

The inflow is assumed to be calorically perfect and well premixed, and so the chemical reaction can be represented by one-step irreversible heat release model with γ, E_a, and Q. This chemical reaction model is the simplest model and is widely used in predicting certain detonation behavior, such as one-dimensional detonation instability [35,36], cellular structures of the normal detonation [37,38], and instability of oblique detonations [25,26]. It should be noted that the single-step chemical kinetics has its limitation and is known to have an impact in predicting certain detonation behavior (i.e., pathological detonations [39,40]). Considering that the heat release process of this study is oblique-shock-induced combustion as well as the success in predicting salient ODW behaviors from previous studies [13–17,21–26], the one-step irreversible heat release chemical model is adopted. The present simulation uses the dimensionless parameters $E_a = 20$, $Q = 50$, and $\gamma = 1.2$. These are traditionally used in numerical simulations as canonical values to investigate detonation wave phenomena in general, only E_a is decreased to include the effects of the high altitude. Assume that the calorically perfect inflow is the basis for the use of the one-step irreversible heat release model, which neglects the real gas effects and the complexity of chemistry, usually concerning tens of species and hundreds of elemental reactions. Nevertheless, this simple model is sufficient because this study mainly focuses on the shock-induced combustion qualitatively as well as the overall ODW initiation dynamics, and the present computational study benefits from its simplicity.

Inflow conditions are fixed at the freestream values in both the left and upper boundaries of the domain. Outflow conditions extrapolated from the interior are implemented on the right and lower boundaries before the wedge. Slip boundary conditions are used on the wedge surface, which starts from $x = 0.5$ on the lower boundary. Initially, the whole flowfield has uniform density, pressure, and velocities, which are calculated according to M_1 and θ. The preexponential factor k is determined to scale the half-reaction length $L_{1/2}$ to unity, and M_1 is fixed to be 12 in all simulations.

In this investigation, a stationary formation structure corresponding to a given M_1 and θ is first simulated. This stationary structure is then used as the initial condition in the successive transient simulation, with the same M_1 but different θ. It is worth noting that, with this computational approach, the finite time required for the wedge-angle change is not exactly considered. However, in practice, mechanically rotating the angle can occur faster than flowfield evolution. For example, a 6 deg rotation will occur in the order of 10^{-5} s with a motor operating at 10^5 rpm. On the other hand, the heat release process in the normal detonation usually has a characteristic length on the scale of 10^{-2} m, but because of the low density at high altitude and the long inert oblique shock shown in the later figures, the characteristic length of this study is easy to reach the scale of 10^{-1} m. Considering the velocity 10^3 m/s, the flow characteristic time is 10^{-4} s, about one order higher than that of angle variation. Hence, neglecting the finite time required for the wedge-angle change is a reasonable assumption, although some physical details during the finite intermediate time of wedge-angle movement may not be fully captured (e.g., expansion growth and pressure waves generated through the finite time wedge-angle variation). The time instant $t = 0$ thus denotes the start of the new transient simulation in this study to investigate the dynamics of the transition process between structures induced by different instantaneous changes of wedge angle.

III. Numerical Results and Discussion

A. Oblique Detonation Wave Structures and Resolution Study

From the viewpoint of the OSW to ODW transition, there are two types of ODW structures. The abrupt transition is featured by the multiwave point and the smooth one by the curved shock, as shown in Fig. 1. Moreover, previous studies [30,41] demonstrate that the smooth transition with a curved shock appears when considering the

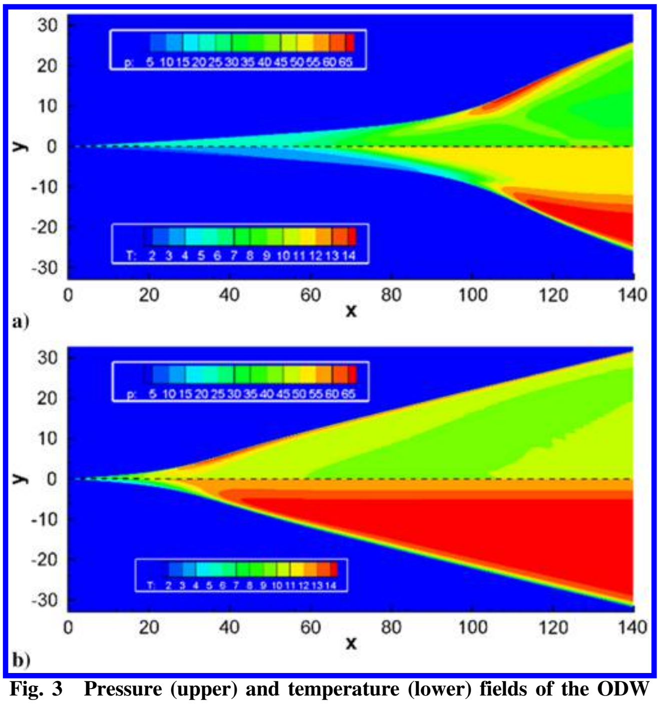

Fig. 3 Pressure (upper) and temperature (lower) fields of the ODW structures with θ equal to a) 18 deg, and b) 24 deg.

inflow conditions of the oblique detonation engines. Results with $\theta = 18$ and 24 deg are shown in Fig. 3, illustrating two structures with the smooth transition, as expected. The OSW–ODW transition can be viewed as the ODW initiation, and the initiation position is found to depend on the wedge angle significantly. With lower θ, the ODW initiation occurs farther downstream, and vice versa. These ODW structures and their dependence on θ agree with previous studies [12–24].

Detonation simulations with different grid sizes are carried out using the same initial and mixture conditions to verify the effect of numerical grid resolution. The pressure contours with 16 and 32 grid points per $L_{1/2}$ of a corresponding CJ detonation are shown in Fig. 4. Only a slight difference of certain pressure contour position is observed, and the flowfields are almost the same for both cases. For

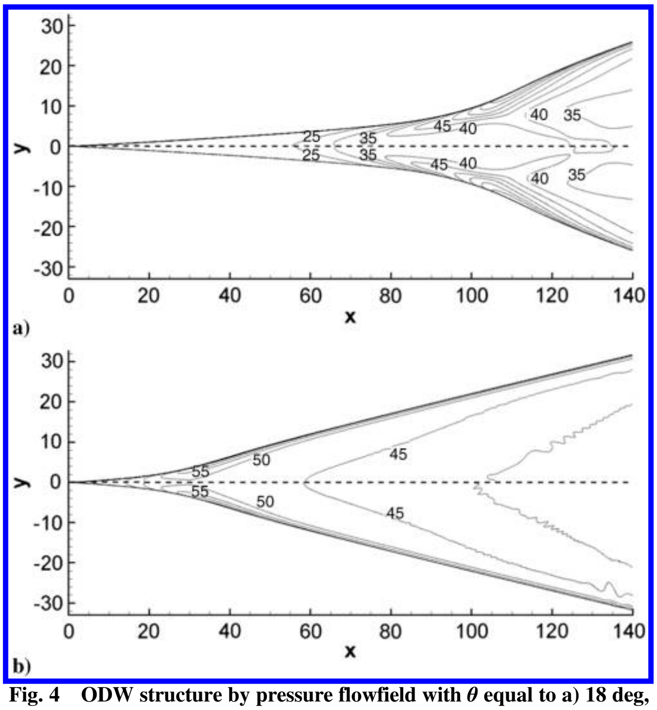

Fig. 4 ODW structure by pressure flowfield with θ equal to a) 18 deg, and b) 24 deg; in each frame, 16 (upper) and 32 (lower) grids per $L_{1/2}$.

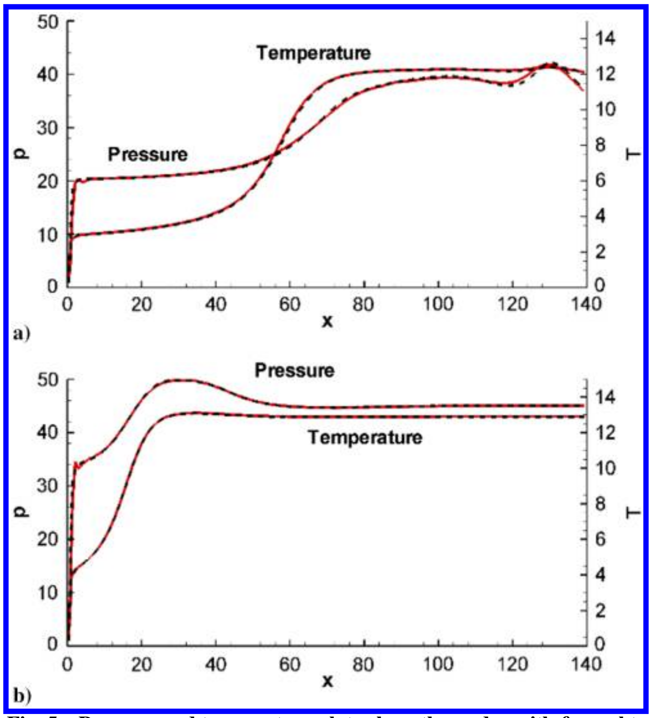

Fig. 5 Pressure and temperature plots along the wedge with θ equal to a) 18 deg, and b) 24 deg; in each frame, 16 (red solid lines) and 32 (black dashed lines) grids per $L_{1/2}$.

better illustration, the corresponding pressure and temperature plots of the two wedge-angle cases along the wedge are also given in Fig. 5, showing good agreement between the results from the two grid resolutions. Furthermore, by examining the reaction progress variable λ, it is found that a numerical resolution of 16 points per $L_{1/2}$ of a CJ detonation equivalently provides about 20 points per $L_{1/2}$ along the x direction for the $\theta = 18$ deg case and 40 points per $L_{1/2}$ for the $\theta = 24$ deg case. This can be thought of as the true resolution to capture the oblique shock and heat release coupling, which is already higher than the resolution used in our previous studies [25,26,41]. This investigation uses the relatively low $E_a = 20$ for considering the inflow conditions of the oblique detonation engines roughly. This makes the change of the reaction progress variable λ relatively less temperature-sensitive, so that cellular structures are absent in the limited computational domain. Previous numerical resolution study [42] has demonstrated that the regular detonation with low activation energy is much easier to converge with fewer grids per half reaction zone. Consequently, a smoother reaction profile can be generated with less numerical grid resolution, and the resolution of 16 grid points per $L_{1/2}$ of a CJ detonation is considered acceptable to simulate the ODW structure with the given parameters in the subsequent simulations.

B. Downstream Transition Induced by Decreasing θ

By decreasing θ from 24 to 18 deg, the ODW structure changes, and the initiation position moves downstream. Theoretically, this will induce the oblique shock angle adjusting slightly from 3.6 to 3.1 deg, but the postshock temperature changes from 4.0 to 2.8. The latter decreases the chemical reaction rate, causing the initiation position to move downstream. Numerical results of the dynamic transition process are shown in Fig. 6. In the initial stage, it is easy to observe the shift of the initiation position toward downstream. As shown in Fig. 6b, a kinklike initiation structure is formed initially, and a local high-density region appears below the OSW. The reaction progress with $\lambda = 0.5$, denoted by the black line, has a spike penetrating into the combustion product, as shown in Fig. 6c. The oblique shock extends farther downstream, generating the high-density region behind the curved shock (Fig. 6d). The structure shown in Fig. 6f approaches to the final stationary configuration as given in Fig. 3a, except the presence of a transverse wave moving downstream along the oblique detonation surface. Generally, the new structure evolves continuously around the original upstream initiation point and then spreads downstream. This flow evolution can be viewed as a global downstream movement of the initiation region. Nevertheless, during the ODW structure evolution, the adjustment to the change of wedge angle is not a simple shift of the complete structure downstream. This leads to a dynamic transition and gives rise to the observed intermediate structure.

Because this study focuses mainly on the dynamic transition of different ODW structures, another resolution study of the transient process is performed, as shown in Fig. 7. The temperature fields show clearly the oblique shock and detonation fronts, the multiwave complex near the transition, and the wave in the combustion product. It is observed that the flowfields are almost the same for both cases,

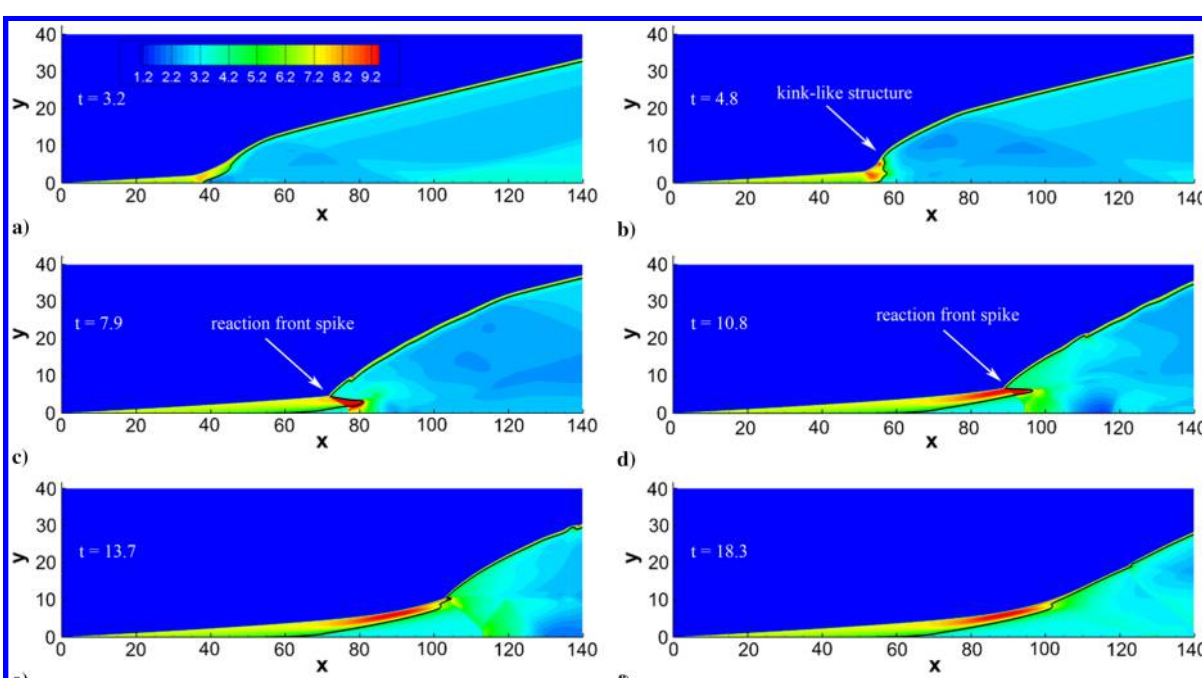

Fig. 6 Evolution of the density field (with black line denoting $\lambda = 0.5$) when θ changes from 24 to 18 deg.

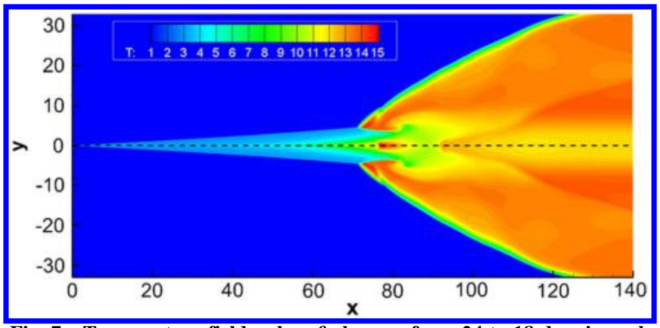

Fig. 7 Temperature fields when θ changes from 24 to 18 deg; in each frame, 16 (upper) and 32 (lower) grids per $L_{1/2}$.

demonstrating that the resolution used here is acceptable to simulate the ODW structure with the given parameters in the subsequent simulations.

To elucidate the temporal features of the observed structure evolution, the initiation length along different lines parallel with the x axis, defined from the oblique shock ($\lambda = 0.0$) to the half reaction surface ($\lambda = 0.5$), are plotted in Fig. 8. The relaxation of the ignition region takes about nondimensional time $t = 5.0$, as shown by the curve along $y = 0$, whereas the evolution of the whole flowfield takes $t > 15.0$. The initiation length along $y = 0$, which corresponds the wedge surface shown by dashed curve, is found to converge quickly. Initially, it moves downstream slowly, but an obvious acceleration can be observed after $t = 1.5$; before it reaches the steady position around $t = 5.0$, a gradual deceleration stage can be observed. Nevertheless, the length variation along $y = 2$ and 4 is found to be more complex where different waves interact. For both curves, the length at the initial stage before $t = 1.0$ decreases slightly. Subsequently, the length along $y = 2$ increases faster than that along

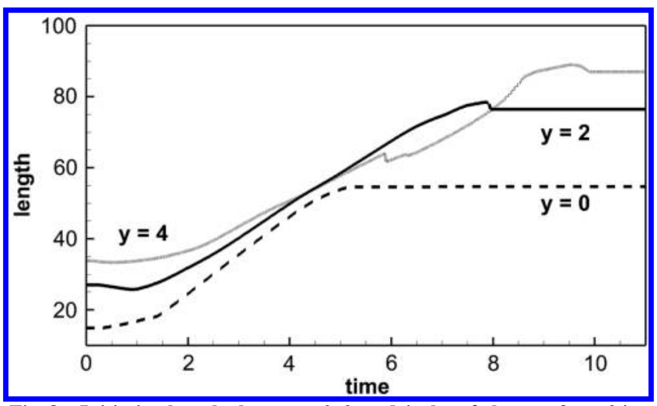

Fig. 8 Initiation length along $y = 0$, 2, and 4 when θ changes from 24 to 18 deg.

$y = 4$, and so the two curves intersect with each other. This can be explained by Figs. 6c and 6d, in which the length along $y = 2$ becomes larger than that along $y = 4$, generating the spike on the half reaction surface. Nevertheless, the length along $y = 2$ soon reaches its final position while the latter length along $y = 4$ increases further, yielding the second intersection around $t = 8.0$. Moreover, these two curves show the slight overshoot of their steady positions. Although the overshoot is not significant, it deserves more attention for its potential impact on ODW applications. Formation of the intersection is due to the difference in the angle between the oblique shock and the oblique detonation. The oblique shock is generated by the wedge, whereas the oblique detonation is not only generated by the wedge but also supported by the postshock heat release. It is observed that the oblique shock responses promptly when inflow parameters change, but the oblique detonation responses slowly. Hence, the slow response of oblique detonation should be attributed to the effects of heat release, which induces the overshoot observed in Fig. 6 and previous studies [17].

C. Upstream Transition Induced by Increasing θ

By increasing θ from 18 to 24 deg, the upstream dynamic transition is illustrated in Fig. 9, showing a different evolution process of the ODW initiation. Because of an increasing θ, the postoblique shock temperature and density rise accordingly, and Fig. 9a shows the high-density region close to the wedge tip. Subsequently, a new, isolated explosion region forms, denoted by the half reaction surface in Fig. 9b. At the same time, the initial reaction surface propagates upstream along the oblique wave, generating a corrugated reaction front into the premixed mixtures. The isolated explosion region soon combines with the upstream propagating reaction surface, generating a merged shock/reaction surface nearly parallel with the wedge, as shown in Fig. 9c. This merged structure featured by the parallel surface is unsteady and responds to the inflow by increasing the oblique detonation angle, as shown in Fig. 9d. The ODW structure eventually relaxes to be that shown in Fig. 3b.

To analyze the formation of the explosion region and related shock/reaction coupling, the evolution of the reaction progress λ on the wedge is shown in Fig. 10a. The initial black curve increases monotonically behind the oblique shock, but a λ peak forms around $x = 12$ at the time instant $t = 1.1$, shown by the red curve (part of the upstream curves is overlapped by the successive curves). Then, the λ peak grows gradually, but its upstream part stays the same, illustrated by the overlaid curves in Fig. 10. The curve trough rises slower than the curve crest, and so the strength of λ peak increases in this period. Generally, the development of the upstream trough should be attributed to the explosion region, and the development of the downstream trough is linked to the original reaction region, which extends upstream due to the inflow variation. The new explosion region manifests during the time $t = 0$ to 2.2, but the propagation of the original reaction region dominates eventually between the time

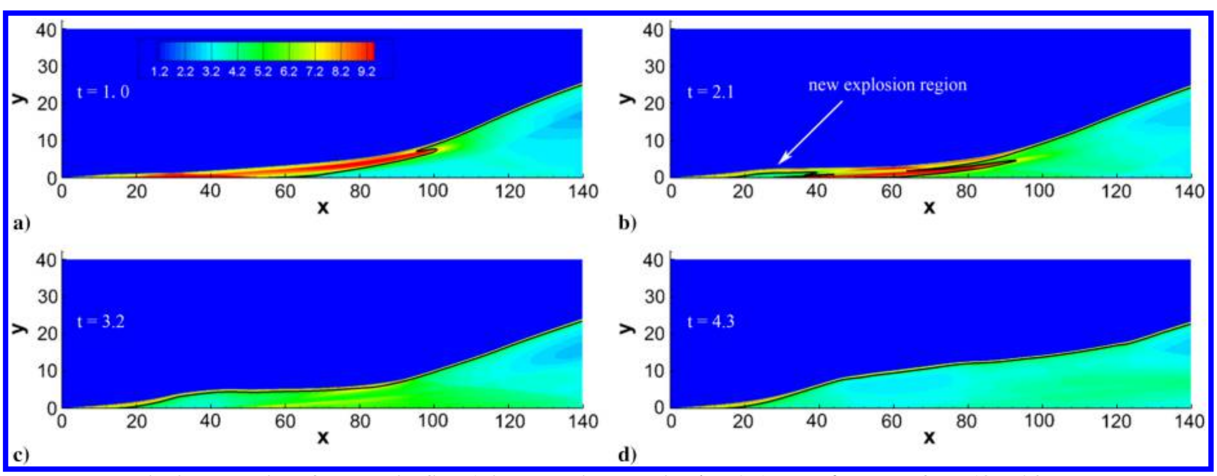

Fig. 9 Evolution of the density field (with black line denoting $\lambda = 0.5$) when θ changes from 18 to 24 deg.

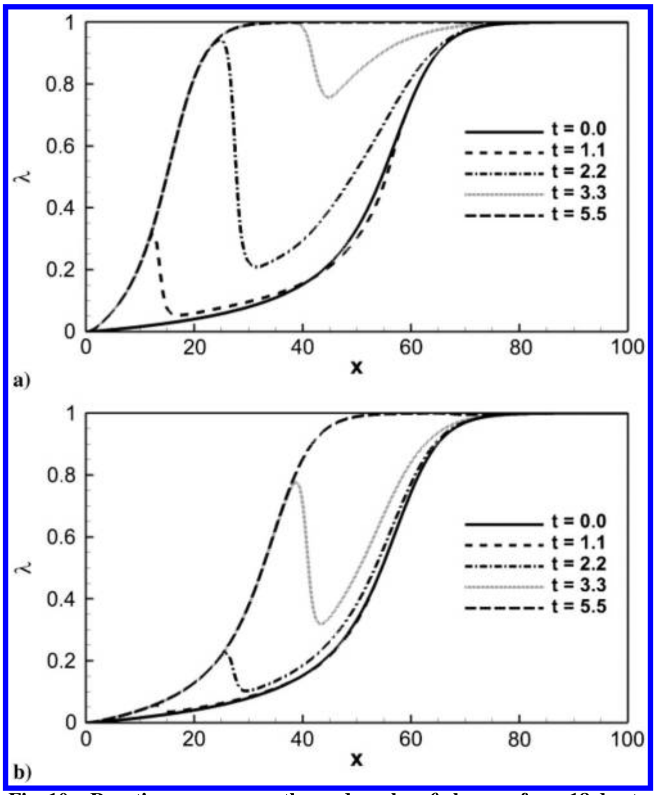

Fig. 10 Reaction progress on the wedge when θ changes from 18 deg to a) 24 deg, or b) 20 deg.

$t = 2.2$ and 5.5. Finally, the new explosion region and the original reaction front merge to establish the final ODW structure.

If the wedge angle increases from 18 to 20 deg, similar phenomena like Fig. 9 can be observed, featured by the formation of the new explosion region. Likewise, the new explosion region merges eventually with the original reaction surface, and the ODW structure relaxes gradually. The evolution of the reaction progress λ on the wedge when θ changes from 18 to 20 deg is plotted in Fig. 10b. The new explosion region appears clearly, but its evolution is slower than the results shown in Fig. 10a. However, the evolution of the original reaction surface becomes much slower, which stays almost the same from $t = 0$ to 3.3. Therefore, the new explosion region plays a more important role in this structural transition, although it is weakened by the small angle increment.

The variation of the initiation length is shown in Fig. 11, with the oblique shock position also given by the dashed line. The steplike change in the initiation length can be observed clearly on the line $y = 0$ and 1, but the shock position changes only on the line $y = 1$. This steplike change is originated from the growth of the discrete,

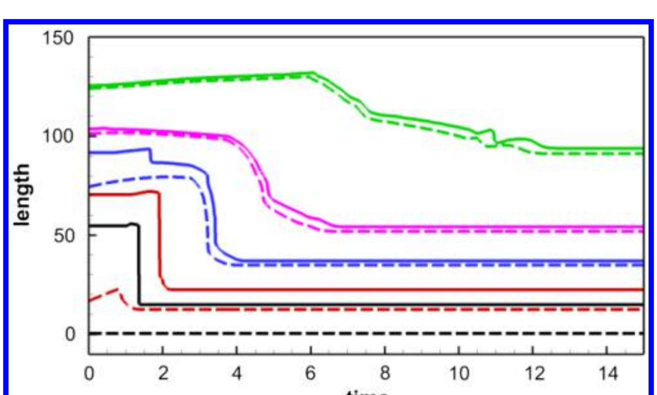

Fig. 11 Initiation length (solid) and shock position (dashed) along $y = 0$ (black), 1(red), 5 (blue), 10 (pink), and 20 (green) when θ changes from 18 to 24 deg.

new explosion region within the original oblique shock beginning from the wedge surface. On the lines $y = 5$, 10, and 20, the effect of the new explosion region becomes progressively less prominent, but several turning points can still be observed clearly.

The formation of the new explosion region only occurs in the upstream transition, which makes the transition complicated and may jeopardize the ODW application from a theoretical point of view. Because the effect of the new explosion region is shown to be weaker if the θ variation is small, as shown in Fig. 10, a case study is performed by controlling the overall θ variation in a quasi-static manner (i.e., to change θ in incremental steps). The results from this idea are shown in Fig. 12a, with an incremental θ change of 2 deg whose start time is denoted by the red arrow (the three red arrows denote that θ changes into 20 deg at $t = 0$, 22 deg at $t = 8$, and 24 deg at $t = 16$, respectively). These results illustrate a smoother change of the initiation length. In such cases, the stepwise behavior is minimized, and the transition region moves upstream gradually toward the final equilibrium position. Meanwhile, the equilibrium oblique detonation in turn takes a longer time, due to the long-time gradual angle variation, to establish as compared to the case with the angle change from 18 to 24 deg directly (see Fig. 10).

Further investigation on weakening the effects of new explosion region is performed by using smaller θ increment and time interval. Generally, we found out that the upstream flowfields are easy to converge, but the downstream flowfields take a relatively long time. Considering that further θ variation will change the downstream flowfields further, the convergence of the downstream flowfields is not necessary. Therefore, another case with an incremental angle change of 1 deg and a short time interval of 2 is simulated, and the corresponding variation of the initial length is shown in Fig. 12b. It is observed that the variation with small angle change and short time interval induce a smoother transition process, and the steplike change in the initiation length becomes weak. Nevertheless, the relaxation process still requires a more significant time to complete than that of the case with θ changing from 18 to 24 deg directly. The balance of the angle change and relaxation time thus needs to be taken into consideration in the actual ODW engine operation.

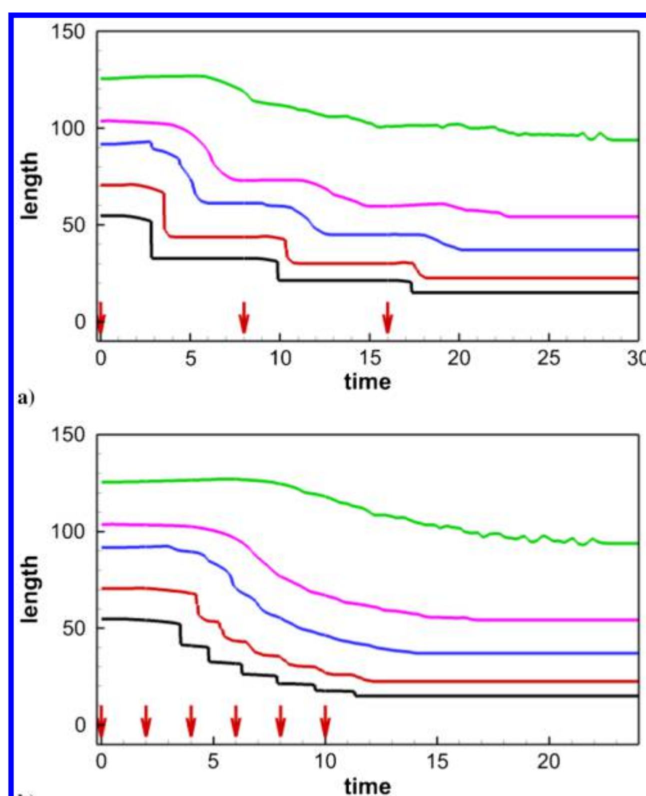

Fig. 12 Initiation length along $y = 0$ (black), 1 (red), 5 (blue), 10 (pink), and 20 (green) when θ changes from 18 to 24 deg, with the increment a) 2 deg, and b) 1 deg.

IV. Conclusions

In this study, the dynamics of the transition between two smooth ODW initiation structures with a curved shock induced by a semi-infinite wedge at high-Mach-number regime is investigated using numerical simulations. Specifically, this study aims to observe the unsteady evolution of the ODW structure and flowfield in response to a wedge-angle variation. By reducing the wedge angle, hence decreasing the strength of the oblique shock and reaction rate, the initiation position and transition process move downstream. The process is referred as "downstream transition". On the other hand, "upstream transition" is the process when the wedge angle increases (causing a higher postoblique shock temperature accordingly), and the ODW formation occurs closer to the wedge tip.

In the downstream transition, the change evolves around the original initiation point, and the overall structure appears to move globally toward the final downstream location. Even though both the original and final stationary structures have the curved-shock configuration for the given flow conditions, a kinklike initiation structure, which is thought to be a more complicated structure, is observed intermediately during the transition process. Furthermore, different parts of the ODW structure reach their equilibrium positions at different time instants. The upstream part, mainly the oblique shock wave without local heat release, always converges first, and the downstream part takes a longer time to converge.

In the upstream transition, an interesting distinct transition pattern appears that induces different wave dynamics. It is featured by a complex evolution with the formation of a new isolated reaction region, a corrugated reaction surface from the original initiation point, a transient coupled shock-reaction surface parallel to the wedge, and its acceleration to establish the new structure corresponding to the new wedge angle. The formation of the new structure concerns two factors; one is the downstream extent of the new explosion region, and the other is the upstream extent of the original reaction surface. With a small angle variation, namely from 18 to 20 deg, the effects of the new explosion region become weak but still dominate the initiation process. It is also observed that the upstream transition with an immediate angle change from 18 to 24 deg generates a steplike variation in the initiation length, mainly caused by the formation of the new reaction region. To minimize this steplike behavior, varying the wedge angle in a quasi-static manner over a finite relaxation time is suggested, and a smoother transition in term of the initiation length variation can be achieved.

These two transient processes demonstrate that the evolutions of the ODW flowfields are irreversible, and two different evolution paths are observed. From another viewpoint, the wedge-angle variation will make the OSW rebuilding first, and then a relatively slower response (convergence) of the combustion region. The transient processes induce the complicated phenomena, like the intermediate kinklike initiation structure, initiation length overshoot, new explosion region, and so on, which is helpful in deepening knowledge on the flow in ODW engines. More fundamental studies on the transient process are thus necessary in the future.

Acknowledgments

The research is supported by the National Natural Science Foundation of China (grant numbers 91641130, 51376165, and 11372333) and the Natural Sciences and Engineering Research Council of Canada.

References

[1] Menees, G. P., Adelman, H. G., Cambier, J., and Bowles, J. V., "Wave Combustors for Trans-Atmospheric Vehicles," *Journal of Propulsion and Power*, Vol. 8, No. 3, 1992, pp. 709–713. doi:10.2514/3.23536

[2] Yi, T. H., Lu, F. K., Wilson, D. R., and Emanuel, G., "Numerical Study of Detonation Wave Propagation in a Confined Supersonic Flow," *Shock Waves*, Vol. 27, No. 3, 2017, pp. 395–408. doi:10.1007/s00193-016-0666-8

[3] Fan, H. Y., and Lu, F. K., "Numerical Modelling of Oblique Shock and Detonation Waves Induced in a Wedged Channel," *Proceedings of the Institute of Mechanical Engineers, Part G: Journal of Aerospace Engineering*, Vol. 222, No. 5, 2008, pp. 687–703. doi:10.1243/09544100JAERO273

[4] Lu, F. K., Fan, H. Y., and Wilson, D. R., "Detonation Waves Induced by a Confined Wedge," *Aerospace Science and Technology*, Vol. 10, No. 8, 2006, pp. 679–685. doi:10.1016/j.ast.2006.06.005

[5] Gross, R. A., "Oblique Detonation Waves," *AIAA Journal*, Vol. 1, No. 5, 1963, pp. 1225–1227. doi:10.2514/3.1777

[6] Pratt, D. T., Humphrey, J. W., and Glenn, D. E., "Morphology of Standing Oblique Detonation Waves," *Journal of Propulsion and Power*, Vol. 7, No. 5, 1991, pp. 837–845. doi:10.2514/3.23399

[7] Ashford, S. A., and Emanuel, G., "Wave Angle for Oblique Detonation Waves," *Shock Waves*, Vol. 3, No. 4, 1994, pp. 327–329. doi:10.1007/BF01415831

[8] Emanuel, G., and Tuckness, D. G., "Steady, Oblique, Detonation Waves," *Shock Waves*, Vol. 13, No. 6, 2004, pp. 445–451. doi:10.1007/s00193-003-0222-1

[9] Li, C., Kailasanath, K., and Oran, E. S., "Detonation Structures Behind Oblique Shocks," *Physics of Fluids*, Vol. 6, No. 4, 1994, pp. 1600–1611. doi:10.1063/1.868273

[10] Li, C., Kailasanath, K., and Oran, E. S., "Effects of Boundary Layers on Oblique-Detonation Structures," *31st Aerospace Sciences Meeting*, AIAA Paper 1993-0450, 1993.

[11] Viguier, C., Figueira da Silva, L., Desbordes, D., and Deshaies, B., "Onset of Oblique Detonation Waves: Comparison Between Experimental and Numerical Results for Hydrogen–Air Mixture," *Proceedings of the Combustion Institute*, Vol. 26, No. 2, 1996, pp. 3023–3031. doi:10.1016/S0082-0784(96)80146-9

[12] Figueira da Silva, L., and Deshaies, B., "Stabilization of an Oblique Detonation Wave by a Wedge: A Parametric Numerical Study," *Combustion and Flame*, Vol. 121, Nos. 1–2, 2000, pp. 152–166. doi:10.1016/S0010-2180(99)00141-8

[13] Papalexandris, M. V., "A Numerical Study of Wedge-Induced Detonations," *Combustion and Flame*, Vol. 120, No. 4, 2000, pp. 526–538. doi:10.1016/S0010-2180(99)00113-3

[14] Teng, H. H., and Jiang, Z. L., "On the Transition Pattern of the Oblique Detonation Structure," *Journal of Fluid Mechanics*, Vol. 713, Dec. 2012, pp. 659–669. doi:10.1017/jfm.2012.478

[15] Teng, H. H., Zhao, W., and Jiang, Z. L., "A Novel Oblique Detonation Structure and Its Stability," *Chinese Physics Letters*, Vol. 24, No. 7, 2007, pp. 1985–1988. doi:10.1088/0256-307X/24/7/055

[16] Choi, J. Y., Shin, E. J. R., and Jeung, I. S., "Unstable Combustion Induced by Oblique Shock Waves at the Non-Attaching Condition of the Oblique Detonation Wave," *Proceedings of the Combustion Institute*, Vol. 32, No. 2, 2009, pp. 2387–2396. doi:10.1016/j.proci.2008.06.212

[17] Teng, H. H., Zhang, Y. N., and Jiang, Z. L., "Numerical Investigation on the Induction Zone Structure of the Oblique Detonation Waves," *Computers and Fluids*, Vol. 95, May 2014, pp. 127–131. doi:10.1016/j.compfluid.2014.03.001

[18] Liu, Y., Wu, D., Yao, S. B., and Wang, J. P., "Analytical and Numerical Investigations of Wedge-Induced Oblique Detonation Waves at Low Inflow Mach Number," *Combustion Science and Technology*, Vol. 187, No. 6, 2015, pp. 843–856. doi:10.1080/00102202.2014.978865

[19] Liu, Y., Liu, Y. S., Wu, D., and Wang, J. P., "Structure of an Oblique Detonation Wave Induced by a Wedge," *Shock Waves*, Vol. 26, No. 2, 2016, pp. 161–168. doi:10.1007/s00193-015-0600-5

[20] Teng, H. H., Ng, H. D., and Jiang, Z. L., "Initiation Characteristics of Wedge-Induced Oblique Detonation Wave in a Stoichiometric Hydrogen–Air Mixture," *Proceedings of the Combustion Institute*, Vol. 36, No. 2, 2017, pp. 2735–2742. doi:10.1016/j.proci.2016.09.025

[21] Grismer, M. J., and Powers, J. M., "Numerical Predictions of Oblique Detonation Stability Boundaries," *Shock Waves*, Vol. 6, No. 3, 1996, pp. 147–156. doi:10.1007/BF02510995

[22] Choi, J. Y., Kim, D. W., Jeung, I. S., Ma, F., and Yang, V., "Cell-Like Structure of Unstable Oblique Detonation Wave from High-Resolution Numerical Simulation," *Proceedings of the Combustion Institute*, Vol. 31, No. 2, 2007, pp. 2473–2480. doi:10.1016/j.proci.2006.07.173

[23] Verreault, J., Higgins, A. J., and Stowe, R. A., “Formation of Transverse Waves in Oblique Detonations,” *Proceedings of the Combustion Institute*, Vol. 34, No. 2, 2013, pp. 1913–1920. doi:10.1016/j.proci.2012.07.040

[24] Teng, H. H., Jiang, Z. L., and Ng, H. D., “Numerical Study on Unstable Surfaces of Oblique Detonations,” *Journal of Fluid Mechanics*, Vol. 744, April 2014, pp. 111–128. doi:10.1017/jfm.2014.78

[25] Teng, H. H., Ng, H. D., Li, K., Luo, C. T., and Jiang, Z. L., “Evolution of Cellular Structures on Oblique Detonation Surfaces,” *Combustion and Flame*, Vol. 162, No. 2, 2015, pp. 470–477. doi:10.1016/j.combustflame.2014.07.021

[26] Yang, P. F., Ng, H. D., Teng, H. H., and Jiang, Z. L., “Initiation Structure of Oblique Detonation Waves Behind Conical Shocks,” *Physics of Fluids*, Vol. 29, No. 8, 2017, Paper 086104. doi:10.1063/1.4999482

[27] Cambier, J. L., Adelman, H., and Menees, G. P., “Numerical Simulations of an Oblique Detonation Wave Engine,” *Journal of Propulsion and Power*, Vol. 6, No. 3, 1990, pp. 315–323. doi:10.2514/3.25436

[28] Vlasenko, V. V., and Sabel’nikov, V. A., “Numerical Simulation of Inviscid Flows with Hydrogen Combustion Behind Shock Waves and in Detonation Waves,” *Combustion, Explosion, and Shock Waves*, Vol. 31, No. 3, 1995, pp. 376–389. doi:10.1007/BF00742685

[29] Iwata, K., Nakaya, S., and Tsue, M., “Wedge-Stabilized Oblique Detonation in an Inhomogeneous Hydrogen–Air Mixture,” *Proceedings of the Combustion Institute*, Vol. 36, No. 2, 2017, pp. 2761–2769. doi:10.1016/j.proci.2016.06.094

[30] Zhang, Y. N., Gong, J. S., and Wang, T., “Numerical Study on Initiation of Oblique Detonations in Hydrogen–Air Mixtures with Various Equivalence Ratios,” *Aerospace Science and Technology*, Vol. 49, Feb. 2016, pp. 130–134. doi:10.1016/j.ast.2015.11.035

[31] Fusina, G., Sislian, J. P., and Parent, B., “Formation and Stability of near Chapman–Jouguet Oblique Detonation Waves,” *AIAA Journal*, Vol. 43, No. 7, 2005, pp. 1591–1604. doi:10.2514/1.9128

[32] Fang, Y. S., Hu, Z. M., Teng, H. H., Jiang, Z. L., and Ng, H. D., “Numerical Study of Inflow Equivalence Ratio Inhomogeneity on Oblique Detonation Formation in Hydrogen–Air Mixtures,” *Aerospace Science and Technology*, Vol. 71, 2017, pp. 256–263. doi:10.1016/j.ast.2017.09.027

[33] Dudebout, R., Sislian, J. P., and Oppitz, R., “Numerical Simulation of Hypersonic Shock-Induced Combustion Ramjets,” *Journal of Propulsion and Power*, Vol. 14, No. 6, 1998, pp. 869–879. doi:10.2514/2.5368

[34] Toro, E. F., *Riemann Solvers and Numerical Methods for Fluid Dynamics*, 2nd ed., Springer, Berlin, 1999, pp. 493–530.

[35] Ng, H. D., Higgins, A., Kiyanda, C., Radulescu, M., Lee, J. H., Bates, K., and Nikiforakis, N., “Nonlinear Dynamics and Chaos Analysis of One-Dimensional Pulsating Detonations,” *Combustion Theory and Modelling*, Vol. 9, No. 1, 2005, pp. 159–170. doi:10.1080/13647830500098357

[36] Henrick, A. K., Aslam, T. D., and Powers, J. M., “Simulations of Pulsating One-Dimensional Detonations with True Fifth Order Accuracy,” *Journal of Computational Physics*, Vol. 213, No. 1, 2006, pp. 311–329. doi:10.1016/j.jcp.2005.08.013

[37] Gamezo, V. N., Desbordes, D., and Oran, E. S., “Two-Dimensional Reactive Flow Dynamics in Cellular Detonation Waves,” *Shock Waves*, Vol. 9, No. 1, 1999, pp. 11–17. doi:10.1007/s001930050134

[38] Gamezo, V. N., Desbordes, D., and Oran, E. S., “Formation and Evolution of Two-Dimensional Cellular Detonations,” *Combustion and Flame*, Vol. 116, Nos. 1–2, 1999, pp. 154–165. doi:10.1016/S0010-2180(98)00031-5

[39] Sharpe, G. J., “Linear Stability of Pathological Detonations,” *Journal of Fluid Mechanics*, Vol. 401, Dec. 1999, pp. 311–338. doi:10.1017/S0022112099006655

[40] Sharpe, G. J., and Falle, S. A. E. G., “One-Dimensional Nonlinear Stability of Pathological Detonations,” *Journal of Fluid Mechanics*, Vol. 414, July 2000, pp. 339–366. doi:10.1017/S0022112000008697

[41] Wang, T., Zhang, Y. N., Teng, H. H., Jiang, Z. L., and Ng, H. D., “Numerical Study of Oblique Detonation Wave Initiation in a Stoichiometric Hydrogen–Air Mixture,” *Physics of Fluids*, Vol. 27, No. 9, 2015, Paper 096101. doi:10.1063/1.4930986

[42] Mazaheri, K., Mahmoudi, Y., and Radulescu, M. I., “Diffusion and Hydrodynamic Instabilities in Gaseous Detonations,” *Combustion and Flame*, Vol. 159, No. 6, 2012, pp. 2138–2154. doi:10.1016/j.combustflame.2012.01.024